

## Numerical Study of Heat Transfer in a Fully Developed Turbulent Pipe Flow

S. Saha<sup>1</sup>, C.C. Chin<sup>1</sup>, H.M. Blackburn<sup>2</sup> and A. Ooi<sup>1</sup>

<sup>1</sup>Department of Mechanical Engineering  
 University of Melbourne, Parkville, Victoria 3010, Australia

<sup>2</sup>Department of Mechanical and Aerospace Engineering  
 Monash University, Victoria 3800, Australia

### Abstract

Direct numerical simulations (DNS) are carried out to investigate fully developed turbulent heat transfer in a pipe at low Kármán number ( $Re_\tau = 171$ ) and different Prandtl numbers ( $Pr = 0.026, 0.1, 0.2, 0.4, 0.71$  and  $1.0$ ) using spectral element method. The isoflux boundary condition is applied on the pipe walls and temperature is considered as a passive scalar. The grid resolution used in the present computation in terms of wall units are  $[\Delta z^+, \Delta r^+, R\Delta\theta^+] = [14.3, 0.5-3.6, 8.4]$ . Important turbulent quantities such as the mean temperature, rms of temperature fluctuations, and both streamwise and radial turbulent heat fluxes are calculated to analyse the effect of Prandtl number. Numerical data from the current computation shows good agreement with other available DNS data, validating the current numerical model.

### Introduction

Over the past ten years, researchers have carried out DNS of turbulent heat transfer in a pipe because of its importance in a wide range of applications such as heat exchangers, air conditioning systems, combustion chambers and cooling passages. Useful information of blood flow through stenosis arteries where thermal inhomogeneity exists owing to accumulation of macrophages or inflammatory cells on plaques can also be obtained from such simulations. Turbulent heat transfer is usually more difficult to study because of its dependence on both Prandtl and Reynolds numbers. DNS at high  $Re$  requires very fine resolution to capture all turbulent length scales; however numerical computation with passive scalars at high  $Pr$  is even more challenging due to the thickness of the thermal boundary layer. The ratio of thermal boundary layer ( $\delta_t$ ) to the velocity boundary layer ( $\delta_v$ ) is  $\delta_t/\delta_v \sim Pr^{-1/3}$ . Thus, the thermal boundary layer is a factor of 2 thinner than the velocity boundary layer at  $Pr = 10$ .

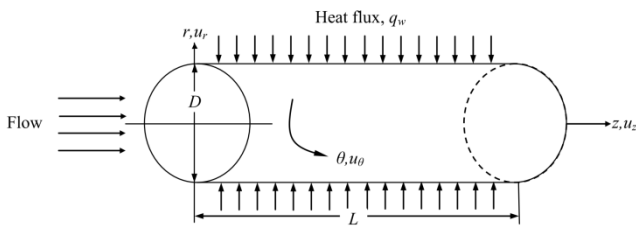


Figure 1. Physical model of the present problem along with the coordinate systems.

Many researchers have carried out DNS of the velocity field at high  $Re$  for both channel and pipe flows. However, a literature survey reveals that DNS of turbulent heat transfer in pipe flows is scarce. The present paper presents data of lower and higher order thermal statistics of turbulent heat transfer in a smooth pipe (figure 1) for different  $Pr$  (i.e. liquid-metal and gases as the

working fluids). A summary of the current study compared with many other DNS data is shown in table 1.

DNS Studies	$L/D$	$\Delta z^+$	$\Delta r^+$	$R\Delta\theta^+$	$Re_D$	$Re_\tau$	Method	$Pr$
Present	$2\pi$	14.3	0.5-3.6	8.4	5000	171	SEM	0.026, 0.1, 0.2, 0.4, 0.71, 1.0
Satake and Kunugi [3]	7.5	10.5	0.29-1.04	8.84	5300	180	FVM	0.71
Piller [4]	6.33	7.03	-	6.28	5300	180	FVM	0.71
Redjem-Saad <i>et al.</i> [5]	7.5	20	0.01-7	10	5500	186	FDM	0.026
	7.5	10	0.01-5	10	5500	186	FDM	0.1, 0.2, 0.4, 0.71, 1.0

Table 1. Comparison of computational condition and grid resolution. ‘+’ denotes the non-dimensional quantities normalised by the friction velocity and the kinematic viscosity.

### Numerical Procedure

The flow is considered as incompressible and neglecting viscous dissipation and buoyancy effect, temperature is modelled as a passive scalar. The dimensionless temperature is defined as  $\Theta = (\langle T_w \rangle - T)/T_r$  where  $T_r = q_w/\rho C_p u_b$  is the reference temperature and  $\langle T_w \rangle$  denotes the wall temperature averaged in time and circumferential direction. The governing equations for flow and passive scalar transport can be expressed in dimensionless forms, using mean velocity,  $u_b$  (ratio of mean volumetric flow rate and pipe cross-sectional area) and diameter of the pipe,  $D$  as velocity and length scales for normalization:

$$\frac{\partial \mathbf{u}}{\partial t} + N(\mathbf{u}) = -\nabla P + \frac{1}{Re_D} \nabla^2 \mathbf{u} + \mathbf{F}, \quad (1)$$

$$\frac{\partial \Theta}{\partial t} + \mathbf{u} \cdot \nabla \Theta - 4u_z = \frac{1}{Re_D Pr} \nabla^2 \Theta, \quad (2)$$

where,  $N(\mathbf{u})$  represents the nonlinear advection terms,  $\mathbf{F}$  is the forcing vector and the bulk Reynolds number,  $Re_D$  is based on bulk velocity  $u_b$  and pipe diameter. The Kármán number,  $Re_\tau$  is defined based on friction velocity  $u_\tau = \sqrt{(\tau_w/\rho)}$  and pipe radius  $R$ . The wall boundary condition is used in the same manner as suggested by Piller [4] that the wall temperature fluctuations are assumed to be zero and  $\Theta = 0$ . The present DNS code is based on spectral element method (SEM) [1] capable to solve these equations with high spatial accuracy.

### Simulation Parameters

The domain length ( $L/D = 2\pi$ ) and resolution has been chosen in accordance with studies conducted by Chin *et al.* [2]. It is discretised by  $15 \times 8$  spectral elements in the meridional semiplane, each consisting of  $10^{\text{th}}$  order Gauss-Lobatto-Legendre (GLL) tensor-product shape function and Fourier expansion

applied with 128 planes of data in the azimuthal direction. A list of comparison of domain length, grid resolution and governing parameters ( $Re_\tau$  and  $Pr$ ) among similar previous DNS [3-5] is presented in table 1. All these previous DNS employed either finite volume method (FVM) or finite difference method (FDM) as the discretisation technique. Turbulent flow is computed from an initial velocity and pressure field supplied by the fully developed flow state obtained by Chin *et al.* [2], while initial thermal field is given as the streamwise velocity component multiplied by the Prandtl number. Simulations are carried out until the ensemble average temperature at the centre of the pipe has converged to a constant value. Statistics are calculated over at least 70 turnover times for all value of Prandtl number considered here.

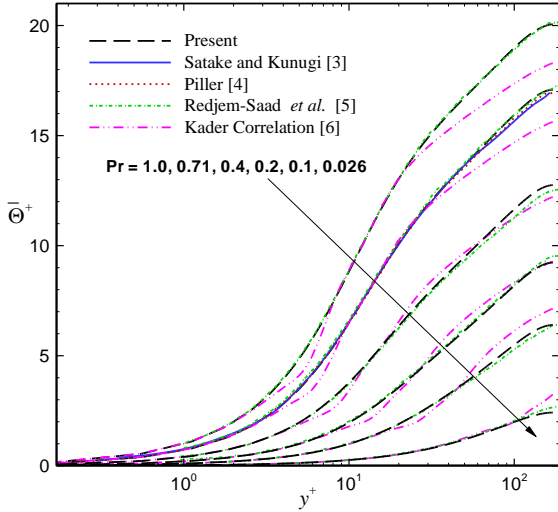


Figure 2. Comparison of mean temperature distribution normalised by friction temperature with other DNS data

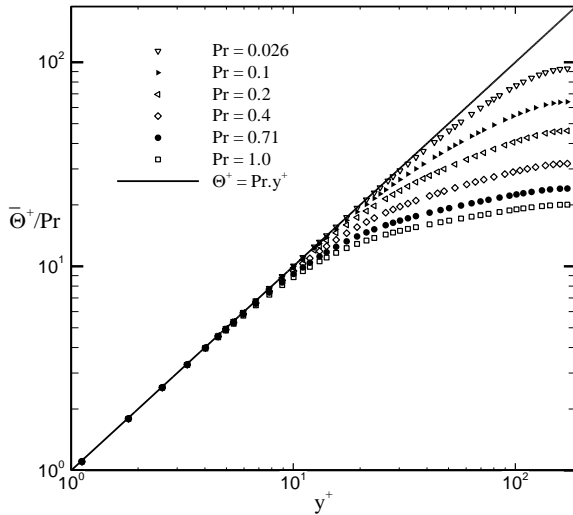


Figure 3. Mean temperature profile with an emphasis on the conduction region

### Mean Temperature Profile

The non-dimensionalised (by friction temperature,  $T_f = q_w/\rho C_p u_\tau$ ) mean temperature profile for various Prandtl numbers. is shown in figure 2. The current results are compared with the empirical equation proposed by Kader [6] and existing DNS data: Satake and Kunugi [3], Piller [4] and Redjem-Saad *et al.* [5]. Despite having slightly different Kármán numbers (see table 1), the overall agreement between present predictions and those obtained by Redjem-Saad is satisfactory. Moreover, the temperature profiles at  $Pr = 0.71$  shows a similar trend for all existing DNS data. It is observed that both present and Piller's computation

have considered shorter pipe than other DNS simulations (see table 1). However, no significant effect of the computational length on mean temperature profile is found, which is consistent with the findings of Chin *et al.* [1], where they reported that mean velocity profile is relatively insensitive to pipe length for  $L/D \geq 2\pi$ . The results agree well with the Kader's correlation from the pipe wall to the edge of logarithmic layer for  $Pr < 0.71$ . At high Prandtl number ( $Pr \geq 0.71$ ), Kader's correlation shows significant discrepancy with all of these DNS computations, mainly in the logarithmic region.

A mean energy balance can be derived by time-averaging equation (2):

$$\frac{1}{Re_\tau Pr} \frac{d}{r dr} \left( r \frac{d\bar{\Theta}^+}{dr} \right) + \frac{d}{r dr} \left( -r u_r'^+ \bar{\Theta}^+ \right) - 4 \frac{\bar{u}_z^+}{U_b^+} = 0. \quad (3)$$

The three terms appearing in the mean heat equation (3), can be interpreted as molecular diffusion transport, turbulent transport, and streamwise mean advection. Mean temperature profiles are characterised by synergetic interaction of these terms, while heat transfer in turbulent flow is generally dominated by turbulent transport. For low  $Pr$ , the magnitude of the molecular diffusion term is always larger than the turbulent transport term. The conductive sublayer then appears to be enlarged and the logarithmic region disappears. As Prandtl number increases, it is expected that there will be larger temperature difference between the wall and the fluid at the pipe cross-section. This is clearly illustrated in figure 3 which shows the behaviour of the mean temperature profiles within the near wall region. All these profiles agree well with the linear profile,  $\bar{\Theta}^+ = Pr y^+$ , in the conductive sublayer ( $y^+ \leq 5$ ). As expected, the conduction region penetrates more deeply into the core region with decreasing Prandtl number.

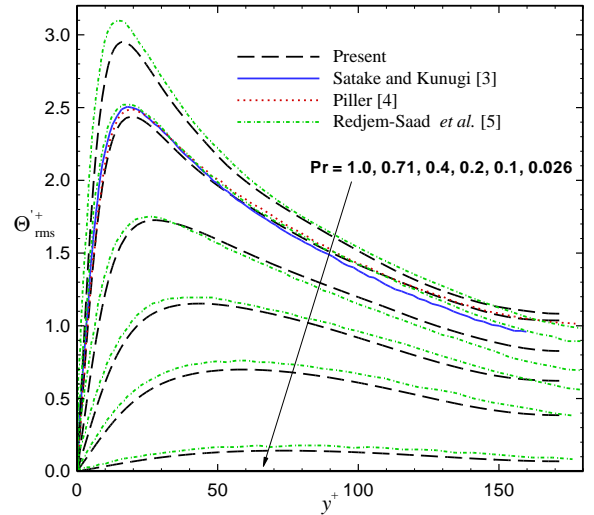


Figure 4. Comparison of RMS values of fluctuating temperature distribution normalised by friction temperature with other DNS.

### Fluctuating Temperature Profile

The root-mean-square temperature fluctuation normalised by the friction temperature is compared with previous results in figure 4 for various Prandtl numbers. Data from the present simulations agree well with DNS data available in the open literature; the main distinctions of the peak value of temperature fluctuation are due to the differences of the Reynolds number and grid resolution. The computational pipe length should be sufficiently long in order to achieve convergence of second order thermal statistics, analogous to the statistics of the velocity field as suggested by Chin *et al.* [1]. At  $Pr = 0.026$ , Redjem-Saad's simulation with coarse streamwise and azimuthal grid resolution also provides higher value of thermal turbulent intensity compared with the present result. Both the present and Piller's

computations follows the same trend at  $Pr = 0.71$ , while Redjem-Saad's data is found to be always higher for  $Pr \geq 0.4$ . Both in the present and other DNS data, the maximum temperature fluctuations are located at  $y^+ \approx 18$  for  $Pr = 0.71$ . With the increase of Prandtl number, the peak temperature variance increases and moves closer to the wall. Kawamura *et al.* [7] in their DNS of turbulent heat transfer in channel flow claimed that the peak value is only a weakly dependent on  $Re_\tau$  for high  $Pr$ . Interestingly, for  $Pr = 1.0$ , the difference of the peak value between the present data and Redjem-Saad's results at the same location ( $y^+ \approx 16$ ) is very significant compare to other Prandtl numbers which seem to contradict the conclusion of Kawamura *et al.* [7]. We propose that this is due to the strong dependence of the peak value on  $Re_\tau$  as is widely accepted by many researchers who have computed turbulent pipe flow [2].

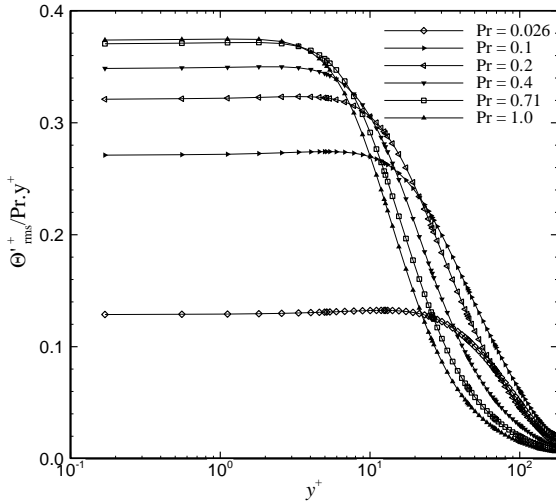


Figure 5. Ratio of  $\Theta'^+_{rms}/Pr y^+$  with an emphasis on the conduction region.

The gradient of the fluctuating temperature  $\Theta'$  over the heated boundary satisfies the following equations

$$\frac{1}{Pr} \frac{d\Theta'^+}{dy^+} = \frac{q'_w}{\bar{q}_w}, \quad (4)$$

where  $\bar{q}_w$  is the average heat flux and  $q'_w$  is its fluctuation. In the vicinity of the wall, it can be expanded usually in terms of  $y^+$  as

$$\Theta'^+ = Pr(b_\theta y^+ + c_\theta y^{+2} + \dots). \quad (5)$$

According to the prediction of Redjem-Saad *et al.* [5],  $b_\theta$  would be independent of  $Pr$  if the Prandtl number is higher than a certain limiting value. This is because for highly conductive fluid, the wall fluctuation  $q'_w$  will tend to zero. Figure 5 shows the evolution of the rms temperature fluctuations which confirms the asymptotic behaviour  $\Theta'^+ \approx b_\theta Pr y^+$  as  $y^+ \rightarrow 0$  to emphasize the near-wall behaviour. The value of coefficient  $b_\theta$  near the wall is estimated to be approximately 0.37 for  $Pr \geq 0.71$  which is slightly lower than the prediction of Redjem-Saad *et al.* [5] ( $b_\theta \approx 0.4$ ). Moreover, when Prandtl number is very low ( $Pr = 0.026$ ), the wall value decreases sharply which is also lower than Redjem-Saad's value mainly due to the difference of  $Re_\tau$  and grid resolution. Although at low  $Pr$ , the general tendency of Reynolds number effect on peak turbulent thermal intensities is small, the coarse resolution used in Redjem-Saad's simulation has a significant impact on the peak value (see Orlandi and Fatica [8] where a grid resolution study on turbulent pipe flow was conducted).

### Streamwise Turbulent Heat Fluxes

The streamwise turbulent heat flux normalized by the friction velocity and temperature is shown in figure 6(a), for different

Prandtl numbers. The overall agreement of the predicted streamwise turbulent heat flux with Redjem-Saad *et al.* [5] is satisfactory. The obvious discrepancy observed at the peak value may be attributed to Reynolds number as explained previously for rms of temperature fluctuations. The dependence of the peak value on the Reynolds number by comparing with Redjem-Saad's results is clearly visible at high  $Pr$ , while Kawamura *et al.* [7] in channel flow simulation observed the opposite behaviour. With the increase of Prandtl number, the conductive sublayer becomes thinner; the peak becomes higher and moves towards the wall. For  $Pr = 0.71$ , the location of the maximum of the streamwise turbulent heat flux is found at  $y^+ \approx 16$ . This value is located between the maximum of rms streamwise velocity fluctuations ( $y^+ \approx 14$ , not shown here) and the maximum of rms temperature fluctuation ( $y^+ \approx 18$ ). Similar observation has been reported in other studies using DNS data. The locations of the peak for  $Pr = 0.2$  and  $1.0$  are  $y^+ \approx 23$  and  $14$ , which are closer to Redjem-Saad *et al.* [5], but their peak point ( $y^+ \approx 57$ ) for  $Pr = 0.26$  is quite different from the present peak location ( $y^+ \approx 48$ ). Near the pipe centre, the streamwise heat flux does not vary with  $Pr$  if  $Pr \geq 0.4$ , similar agreement is also found by Redjem-Saad *et al.* [5].

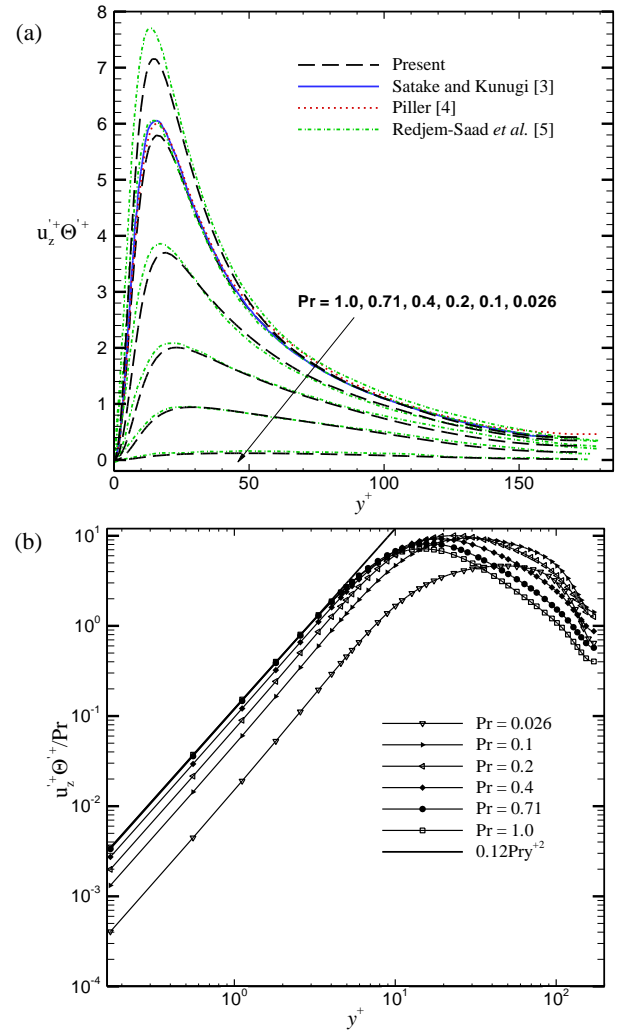


Figure 6. Streamwise turbulent heat flux: (a) comparison with other DNS and (b) the ratio of  $u_z^+ \Theta'^+ / Pr$ .

The ratio of  $u_z^+ \Theta'^+ / Pr$  is plotted in figure 6(b) with emphasis on the near-wall region. As mentioned in Redjem-Saad *et al.* [5], using the expressions of the temperature and velocity fluctuations, streamwise heat flux can be expressed as:

$$\overline{u_r^+ \Theta^+} = Pr(\overline{b_r b_\theta} y^{+2} + \overline{c_r c_\theta} y^{+3} + \dots), \quad (6)$$

where the correlation coefficient  $\overline{b_r b_\theta}$  in the vicinity of the wall is independent of  $Pr$  for  $Pr \geq 0.71$ . The value of  $\overline{b_r b_\theta}$  is about 0.12 which is almost consistent with the Redjem-Saad's value ( $\overline{b_r b_\theta} \approx 0.13$ ).

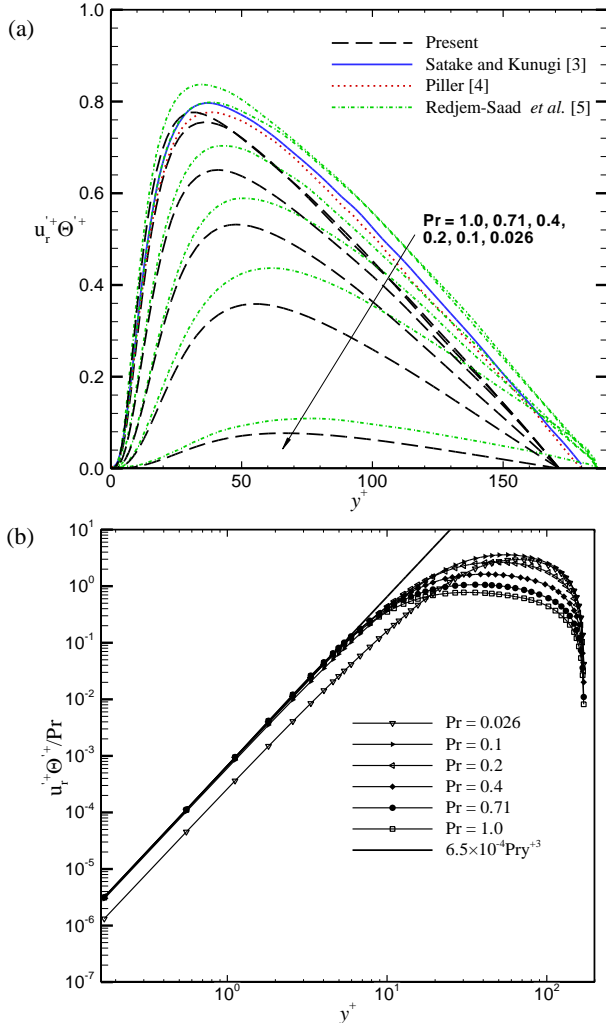


Figure 7. Radial turbulent heat flux: (a) comparison with other DNS and (b) the ratio of  $\overline{u_r^+ \Theta^+} / Pr$ .

### Wall-normal Turbulent Heat Fluxes

The wall-normal turbulent heat flux is plotted in figure 7(a). Over the pipe cross-section, the wall-normal turbulent heat flux is smaller by an order of magnitude when compared to the streamwise turbulent heat flux. Moreover, the wall-normal heat flux reaches a maximum further away from the wall than the streamwise heat flux due to strong damping of the wall-normal velocity fluctuation, which has its maximum at  $y^+ = 53$  (not shown here). Similar to the streamwise heat flux distribution, the present DNS considerably under predicts the wall-normal heat flux than other DNS because of the low  $Re_\tau$ -value. In the vicinity of the wall, the conductive heat flux plays a dominant role, while the turbulent heat flux dominates in the core region. With the increase of the Prandtl number, the radial turbulent heat flux increases which is balanced by the decrease in the conductive heat flux. The peak of the wall-normal turbulent heat flux rises and shifts towards the wall, while due to higher  $Re_\tau$ , as in Redjem-Saad *et al.* [5], the peak shifts away from the wall for the same  $Pr$ . Other than  $Pr$ , the transverse curvature also affects the radial turbulent heat flux as observed in figure 7(b). The distribution of

radial heat flux decreases from the location of the peak point to the pipe centre at zero value for all Prandtl numbers.

Similar to the streamwise heat flux, the wall-normal heat flux can be expressed as:

$$\overline{u_r^+ \Theta^+} = Pr(\overline{b_r b_\theta} y^{+3} + \overline{c_r c_\theta} y^{+4} + \dots), \quad (7)$$

which indicates asymptotic behaviour in the near-wall region as evident in figure 7(b). The wall value of the correlation coefficient  $\overline{b_r b_\theta}$  is about  $6.5 \times 10^{-4}$  which is independent of all  $Pr$  except  $Pr = 0.026$  and also in good agreement with the ones obtained by Redjem-Saad *et al.* [5] ( $\overline{b_r b_\theta} \approx 7.0 \times 10^{-4}$ ).

### Conclusions

The statistical results obtained from DNS of turbulent heat transfer in pipe flow are seen to be in good agreement with data available in the open literature. For low Prandtl number, the logarithmic regions are practically non-existent near the core of the pipe. Future work will include the effect of Reynolds numbers ( $Re_\tau \geq 500$ ) for fluid having high Prandtl number,  $Pr \geq O(1)$ . This will possibly able to give a framework to establish scaling of the temperature profile in a turbulent pipe flow for a wide range of working fluids with different thermal characteristics.

### Acknowledgments

This research was supported by a Victorian Life Sciences Computation Initiative (VLSCI) grant on its Peak Computing Facility at the University of Melbourne, an initiative of the Victorian Government.

### References

- [1] Blackburn, H. M. & Sherwin, S. J., Formulation of a Galerkin Spectral Element – Fourier Method for Three-Dimensional Incompressible Flows in Cylindrical Geometries, *J. Comput. Phys.*, **197**, 2004, 759-778.
- [2] Chin, C., Ooi, A., Marusic, I. & Blackburn, H., Effects of Computation Pipe Length on Turbulence Statistics using DNS of Turbulent Pipe Flow, in *62<sup>nd</sup> Annual Meeting of the APS Division of Fluid Dynamics*, Minneapolis, Minnesota, 2009.
- [3] Satake, S. & Kunugi, T., Direct Numerical Simulation of Turbulent Heat Transfer in an Axially Rotating Pipe Flow: Reynolds Shear Stress and Scalar Flux Budgets, *Int. J. Numer. Meth. Heat Fluid Flow*, **12**(8), 2002, 958-1008.
- [4] Piller, M., Direct Numerical Simulation of Turbulent Forced Convection in a Pipe, *Int. J. Numer. Meth. Fluids*, **49**, 2005, 583-602.
- [5] Redjem-Saad, L., Ould-Rouis, M. & Lauriat, G., Direct Numerical Simulation of Turbulent Heat Transfer in Pipe Flows: Effect of Prandtl Number, *Int. J. Heat Fluid Flow*, **28**, 2007, 847-861.
- [6] Kader, B. A., Temperature and Concentration Profiles in Fully Turbulent Boundary Layers, *Int. J. Heat Mass Transfer*, **24**, 1981, 1541-1544.
- [7] Kawamura, H., Abe, H. & Matsuo, Y., DNS of Turbulent Heat Transfer in Channel Flow with Respect to Reynolds and Prandtl Number Effects, *Int. J. Heat Fluid Flow*, **20**, 1999, 196-207.
- [8] Orlandi, P. & Fatica, M., Direct Simulations of Turbulent Flow in a Pipe Rotating About its Axis, *J. Fluid Mech.*, **343**, 1997, 43-72.